



ALMA MATER STUDIORUM
UNIVERSITÀ DI BOLOGNA

ARCHIVIO ISTITUZIONALE
DELLA RICERCA

Alma Mater Studiorum Università di Bologna
Archivio istituzionale della ricerca

Geophysical Responses to an Environmentally-Boosted Volcanic Unrest

This is the final peer-reviewed author's accepted manuscript (postprint) of the following publication:

Published Version:

De Siena L., Amoruso A., Petrosino S., Crescentini L. (2024). Geophysical Responses to an Environmentally-Boosted Volcanic Unrest. *GEOPHYSICAL RESEARCH LETTERS*, 51(5), 1-11 [10.1029/2023GL104895].

Availability:

This version is available at: <https://hdl.handle.net/11585/973334> since: 2024-07-03

Published:

DOI: <http://doi.org/10.1029/2023GL104895>

Terms of use:

Some rights reserved. The terms and conditions for the reuse of this version of the manuscript are specified in the publishing policy. For all terms of use and more information see the publisher's website.

This item was downloaded from IRIS Università di Bologna (<https://cris.unibo.it/>).
When citing, please refer to the published version.

(Article begins on next page)

Geophysical responses to an environmentally-boosted volcanic unrest

De Siena, L.^{1,2,3}, Amoruso A.^{4,*}, Petrosino S.⁵, Crescentini L.⁴

¹ *Institute of Geosciences, Johannes Gutenberg University, Mainz, 55128, Germany.*

² *TeMaS - Terrestrial Magmatic Systems Research Area, Johannes Gutenberg University, Mainz, 55128, Germany.*

³ *Department of Physics and Astronomy "Augusto Righi", Alma Mater Studiorum, Bologna, 40127, Italy.*

⁴ *Department of Physics, University of Salerno, Fisciano, 84084, Italy.*

⁵ *Istituto Nazionale di Geofisica e Vulcanologia, Sezione di Napoli - Osservatorio Vesuviano, Napoli, 80124, Italy.*

*gamoruso@unisa.it

Contents of this file

Text S1

Table S1

Figures S1 to S10

Introduction

Text S1 clarifies which stations have been used in each period considered through the main text. Table S1 shows the yearly average rainfall recorded by the 3Bmeteo dataset for the Pozzuoli station. Figure S1 shows the time series presented in the article over the longest available period and compares them to rainfalls over hydrological years. Fig. S2, S4 and S5 show different steps of the MEOF and results obtained before and after processing. Fig. S3 shows the same results in the main text at the broader caldera scale. Figs. S6 and S7 show the secondary EOF components with earthquake locations through time, used to define seismic migrations and fronts. Fig. S8 compares CO₂ emissions at Solfatara and Pisciarelli. Fig. S9 shows seismic migrations acting in 2019 around the central supercritical fluid reservoirs from different directions. Fig. S10 shows the contribution of each component when considering the 2012-2022 weekly time series.

Text S1

The MEOF analysis requires the data from the different stations to be simultaneous. Because the time series of the different stations start at different times and have non-coincident breaks, we used the stations listed below for the different time periods analyzed.

- From 2013 to 2019: ARFE, BAIA, FRUL, IPPO, LICO, MAFE, MORU, QUAR, RITE, SOLO, STRZ, VICA;
- From 2014 to 2019: ARFE, BAIA, FRUL, IPPO, LICO, MAFE, MORU, QUAR, RITE, SOLO, STRZ, VICA;
- From 2016 to 2019: ARFE, BAIA, CMIS, FRUL, IPPO, ISMO, LICO, MAFE, MORU, NAMM, QUAR, RITE, SOLO, STRZ, VICA;
- From 2013 to 2022: ARFE, BAIA, FRUL, IPPO, LICO, MORU, QUAR, RITE, SOLO, STRZ, VICA (weekly data).

Hydrological (September-August)	Year	Cumulative Rainfall (mm)	Season drought
2012-2013		2335	Wet
2013-2014		2040	Wet
2014-2015		2176	Wet
2015-2016		1513	Dry
2016-2017		1123	Very Dry
2017-2018		2349	Wet
2018-2019		1386	Dry
2019-2020		1354	Dry
2020-2021		2376	Wet
2021-2022		1543	Dry
2022-2023		1053	Very Dry

Table S1. Average rainfall during the hydrological year as recorded by the 3Bmeteo dataset for the Pozzuoli station.

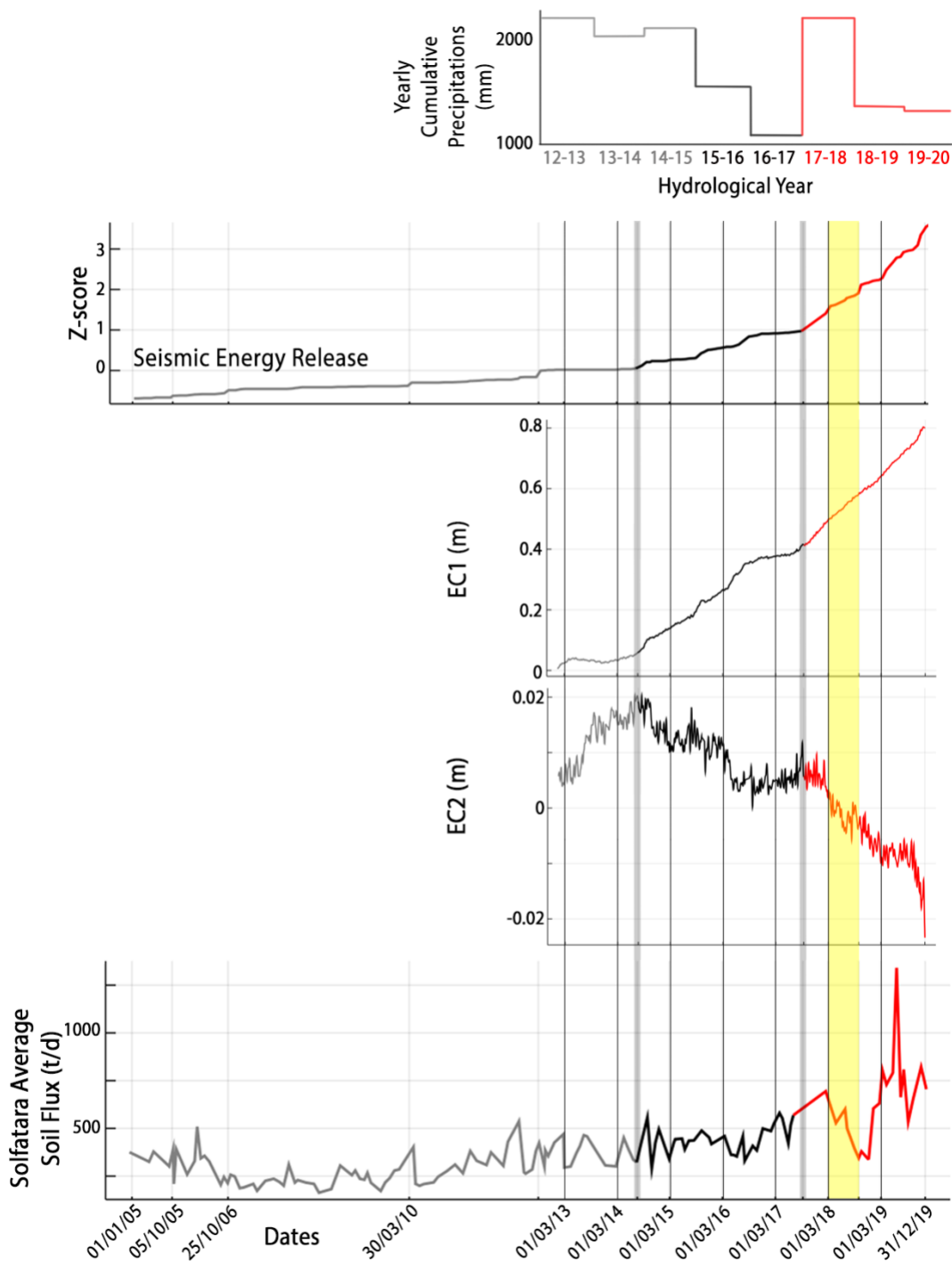


Figure S1. Relationship between precipitations (bar chart), seismic, EC1, EC2 and geochemical (lines) information. The grey, black, and red periods show different trends in seismic energy with progressively longer seismic releases through time (grey= \sim 1 day; black= \sim 1 month; red=continuous).

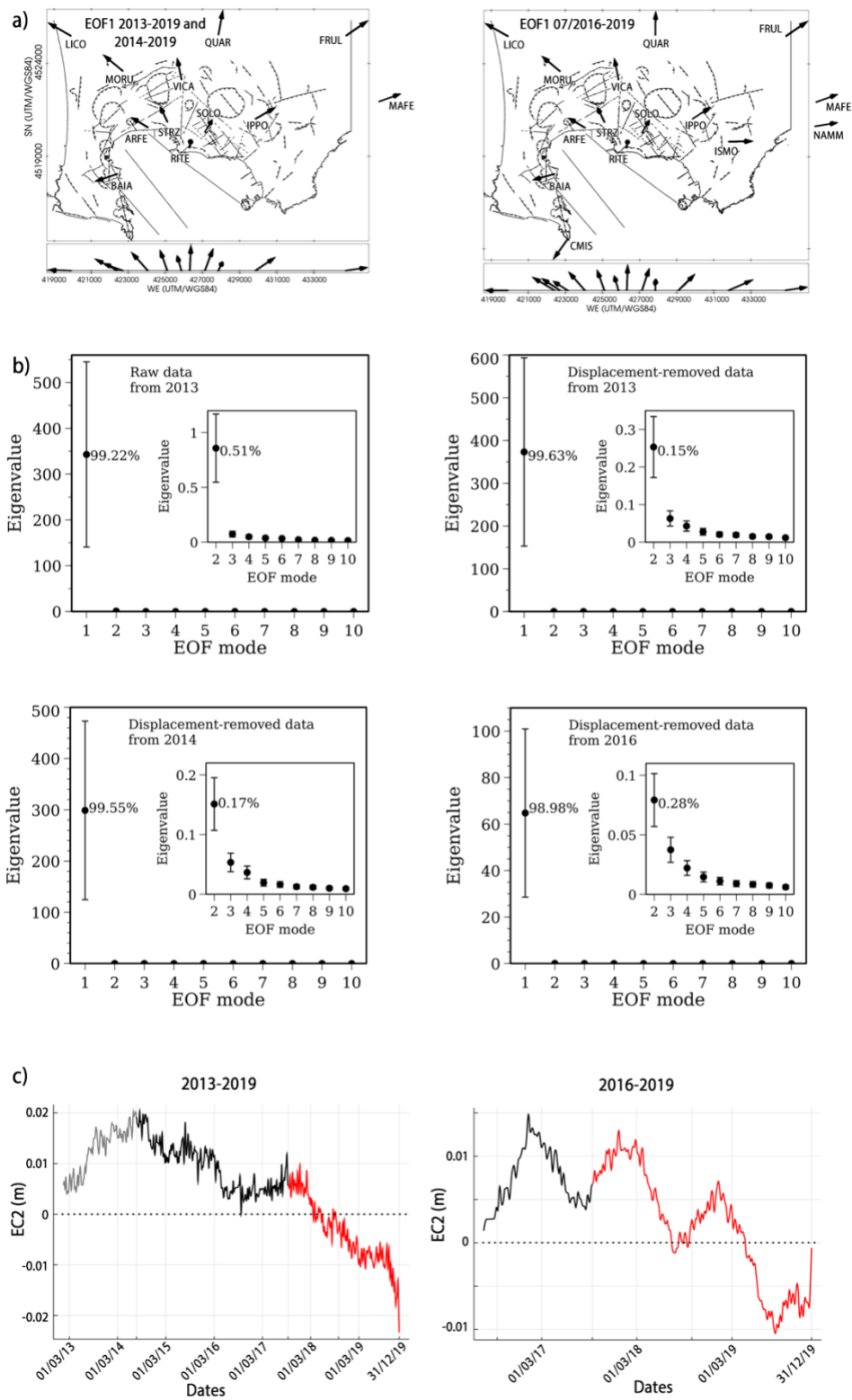


Figure S2. EOFn in two different periods. a) EOF1 patterns computed until December 2019 from January 2013 and July 2014 (same patterns and stations) and July 2016, when additional stations were available. b) Eigenvalues with their errors (line plot) and model variance percentage signals (first two eigenvalues) from 2013 (raw and displacement-removed processing), 2014 and 2016. c) EC2 for the two periods not shown in Fig. 1b.

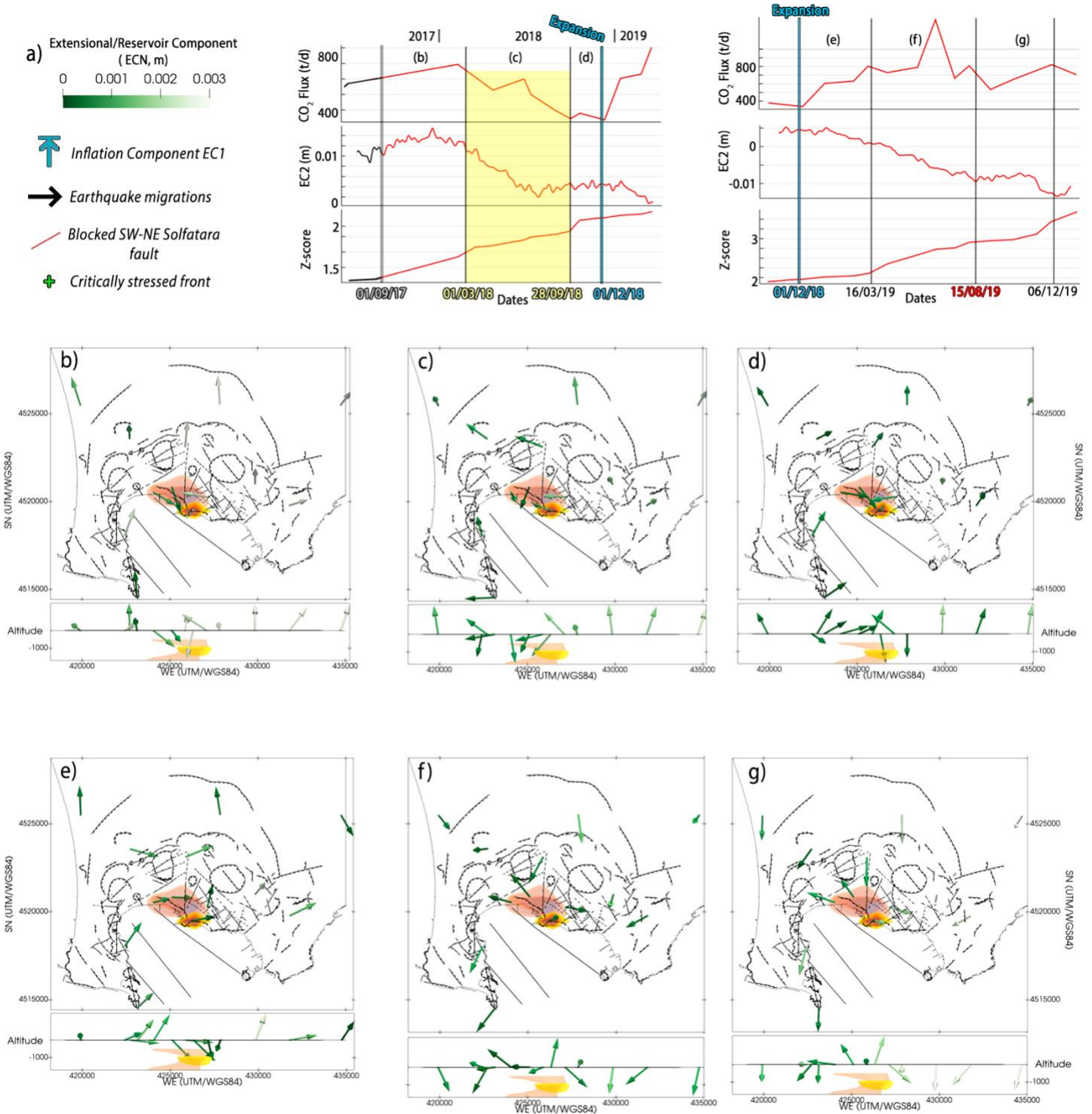


Figure S3. EOFN and ECN patterns from the 2017 extreme rainfall events across the entire caldera. a) CO₂ soil flux, EC2, and seismic energy time series from the 2017 extreme rainfall events to the end of 2019. The legend reports the green colour scale used to display the ECN average deformation in each period in the following panels. b-g) The EOFN and ECN patterns at all stations except MAFE and NAMM (Fig. S2a) in the same periods reported in Figs. 2 and 3.

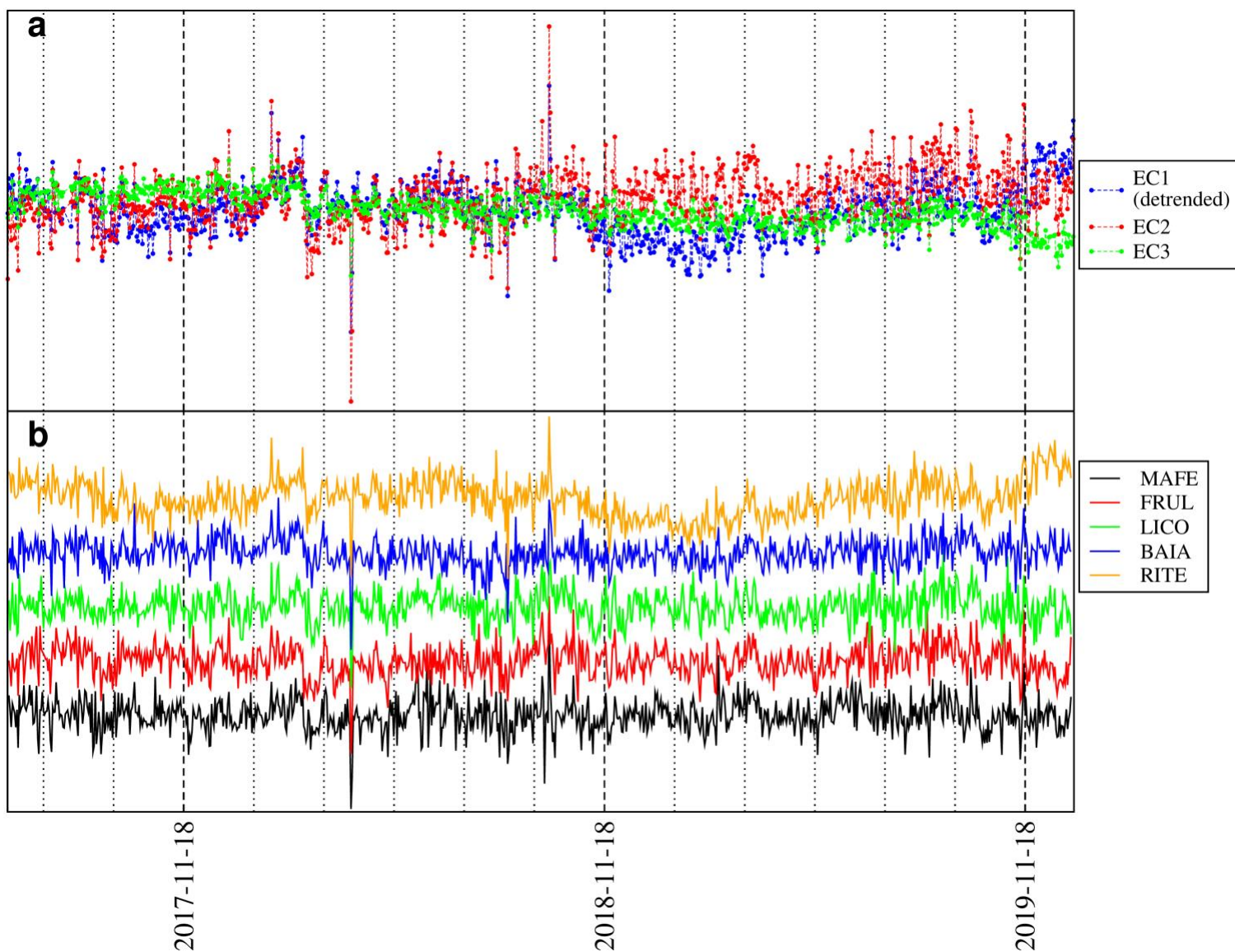


Figure S4. High-frequency signals common to all GPS stations. a) EC_n computed on raw daily data from January 2013 to December 2019; the best-fit linear trend has been removed from EC_1 . b) Daily vertical displacements at five GPS stations, inside and outside the caldera (see map in Fig. S2a); the best-fit linear trend has been removed from each time series.

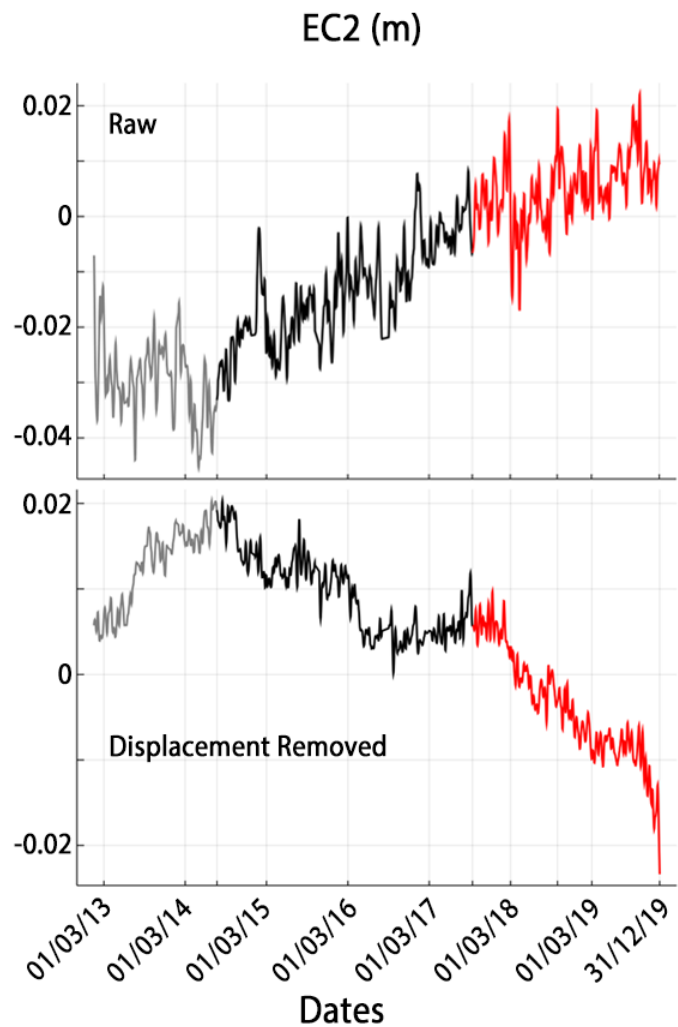
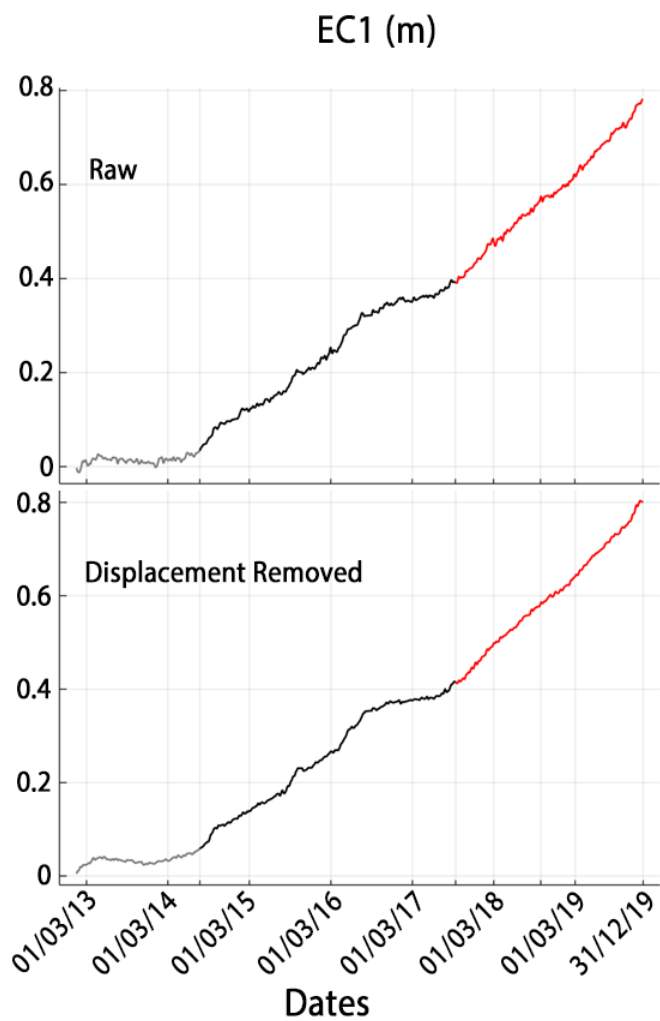


Figure S5. EOF data processing. Time series corresponding to EC1 and EC2 since 2013. The top and bottom rows show the raw and displacement-removed EC_n, respectively.

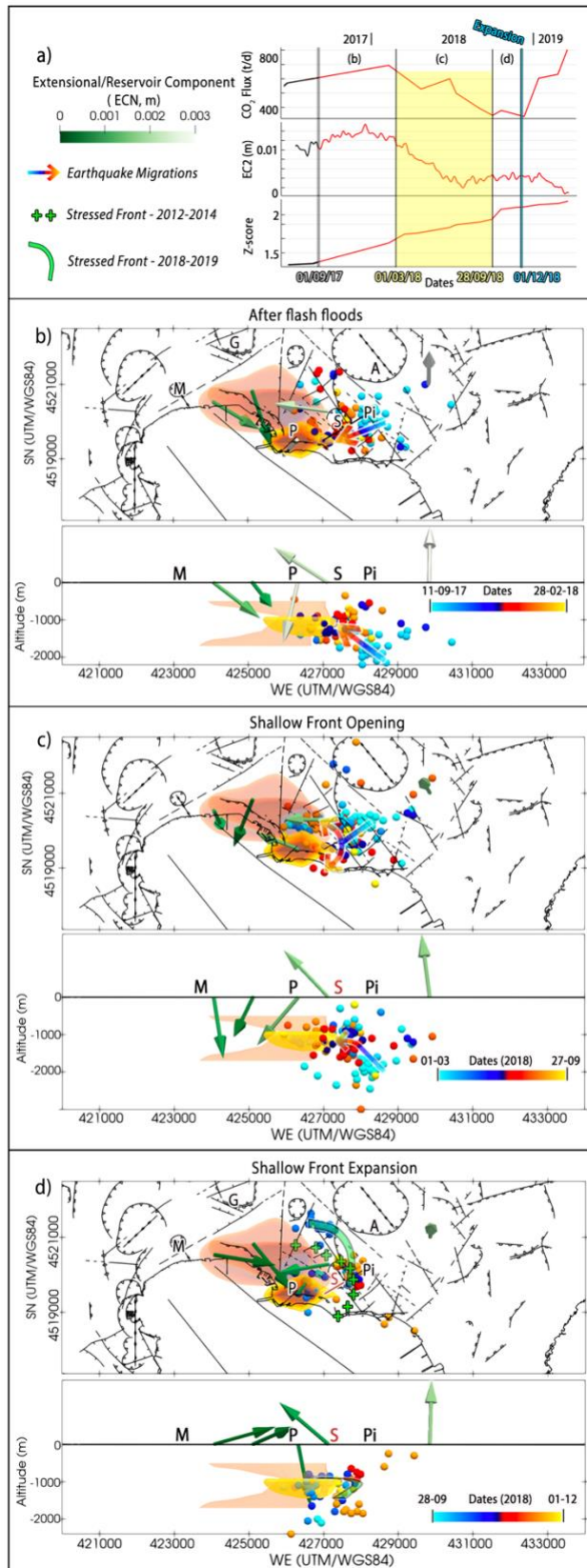


Figure S6. Seismic and secondary deformation patterns before and during the sink. a) CO₂ soil flux, *EC2*, and seismic energy time series from the 2017 rainfall events (Scafetta & Mazzarella, 2021) to the end of the sink. Line colours are identical to those in Fig. 1b. Green colour scale: *ECN* average deformation in each period. b-d) Comparison between the *EOFN* and *ECN* patterns (arrows at the surface and their color), earthquake locations color-scaled depending on nucleation time (from cyan to yellow) and fronts. Seismic migrations and fronts are interpreted from the earthquake spatio-temporal patterns. Solfatarata (**S**) is labelled in red during sink periods and in black otherwise.

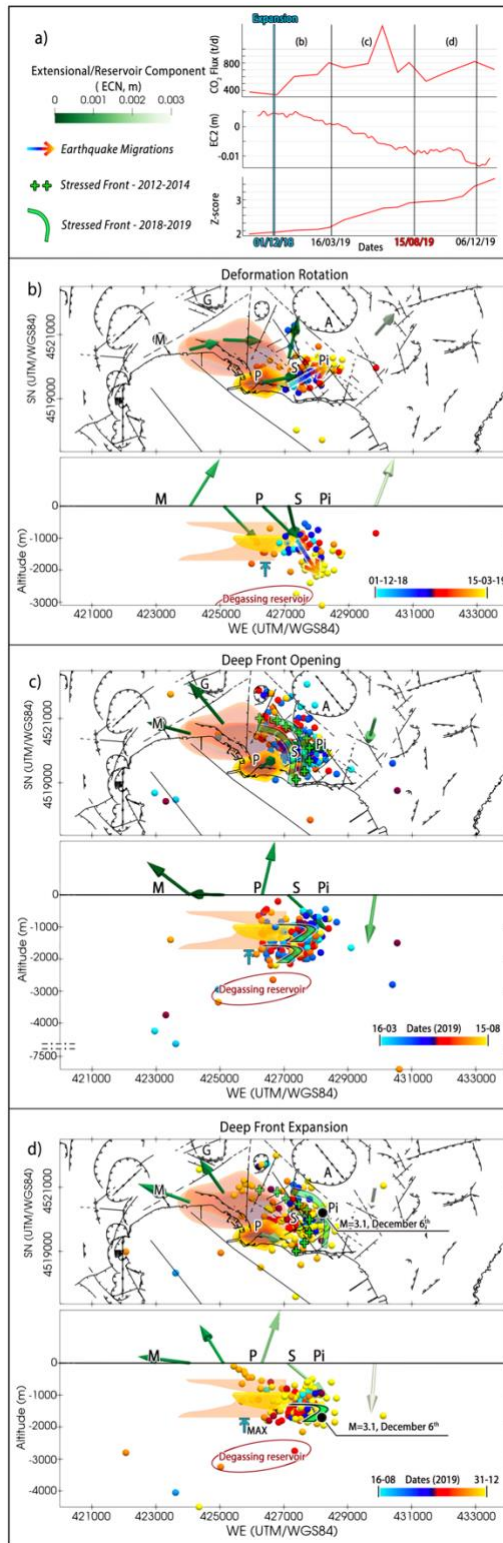


Figure S7. Seismic and secondary deformation patterns after the sink. Same as Fig. S6 for the recovery period from the sink to the end of 2019.

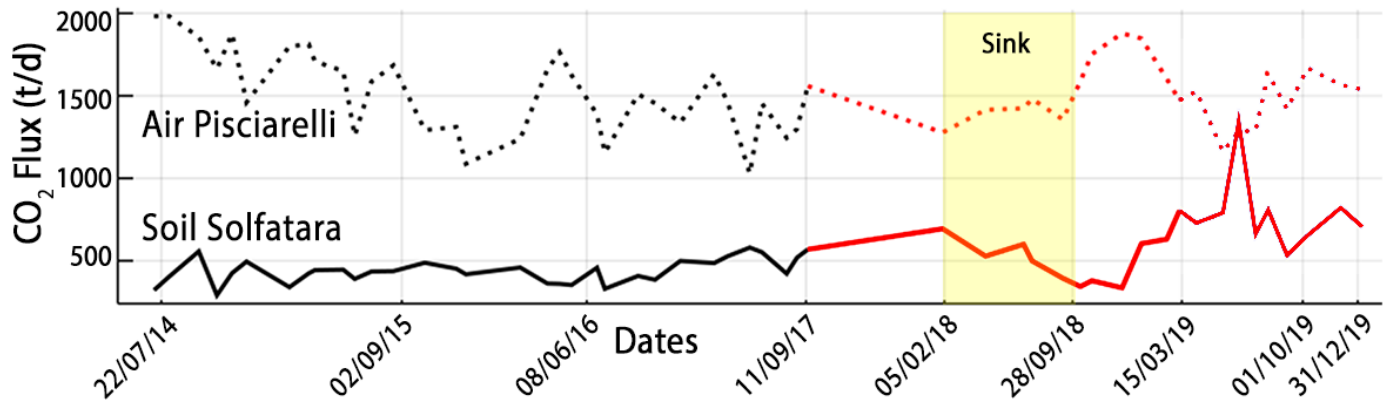


Figure S8. Flux comparisons. Comparison between the time series of soil flux at Solfatara (continuous line) and air flux at Pisciarelli (dotted) from Chiodini et al. (2021).

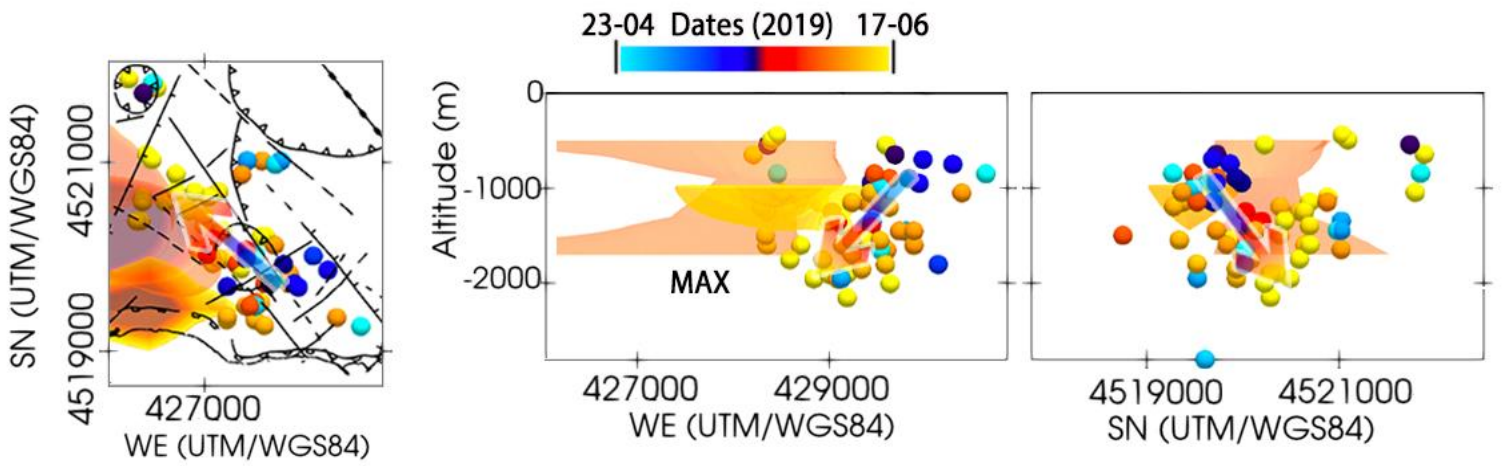


Figure S9. Seismic migrations April-June 2019. Earthquake migrations (arrows are interpreted paths) around the central reservoirs and coloured by date as seen from the top, WE and SN directions.

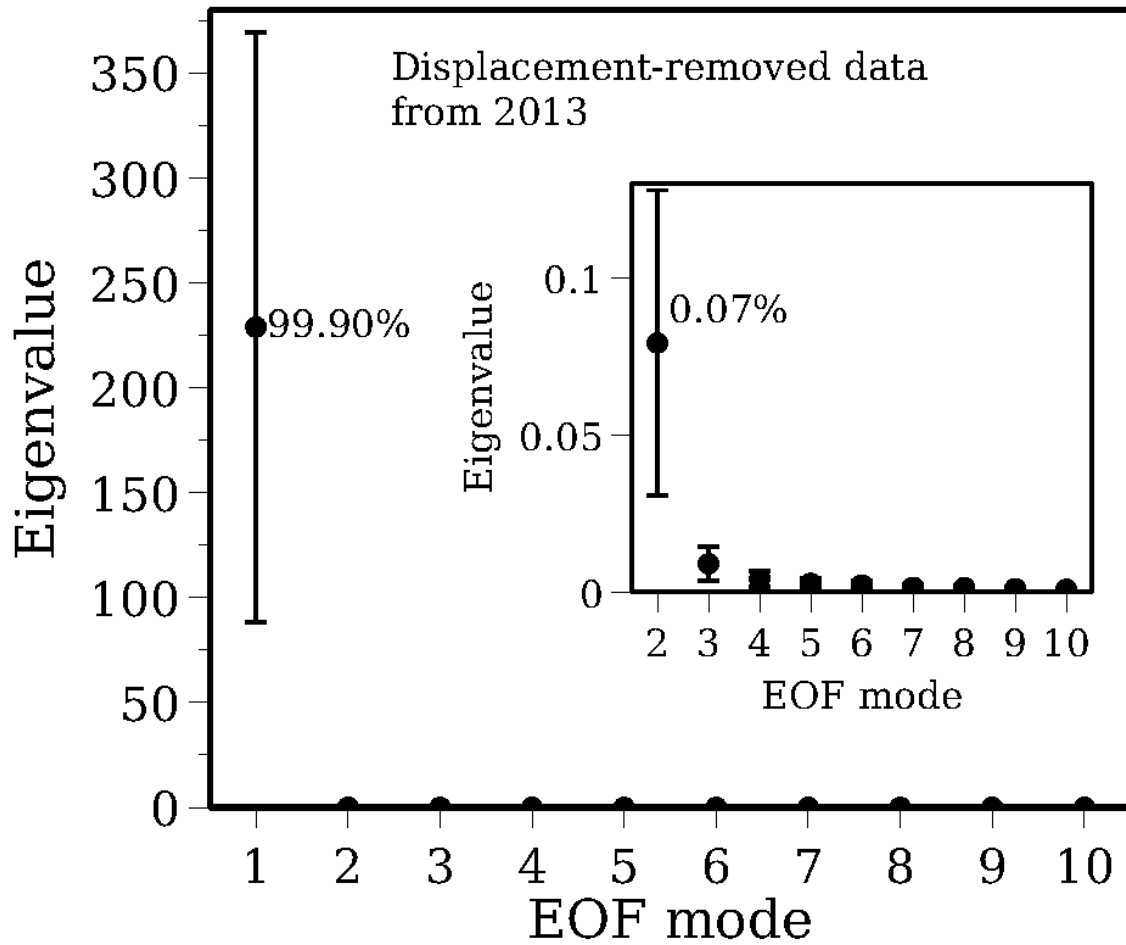


Figure S10. EOF components from weekly January 2013- December 2022 time series. Eigenvalues with their errors (line plot) and model variance percentage signals (first two eigenvalues) computed from weekly data spanning from 2013 to 2022.